Journal of Power Sources 245 (2014) 76–82

Contents lists available at SciVerse ScienceDirect

Journal of Power Sources

journal homepage: www.elsevier.com/locate/jpowsour

# Electrochemical properties of high rate bias sputtered $LiCoO_2$ thin films in liquid electrolyte

S. Tintignac [a,b,1], R. Baddour-Hadjean [a,*], J.P. Pereira-Ramos [a], R. Salot [b]

[a] Institut de Chimie et des Matériaux Paris Est, ICMPE/GESMAT, UMR 7182 CNRS-Université Paris Est Créteil (UPEC), 2 rue Henri Dunant, 94320 Thiais, France
[b] DRT/LITEN/DTNM/LCMS, CEA Grenoble, 17 rue des Martyrs, 38054 Grenoble, France

## HIGHLIGHTS

- Sputtered $LiCoO_2$ thin films were prepared using a bias effect.
- We report the best electrochemical characteristics in liquid electrolyte.
- The bias effect is the key parameter to get high performance films.
- Outstanding cycling stability and high rate capability.
- High electrochemical efficiency: 200 μAh $cm^{-2}$ with a 3.6 μm thick film.

## ARTICLE INFO

*Article history:*
Received 5 October 2012
Received in revised form
7 June 2013
Accepted 7 June 2013
Available online 21 June 2013

*Keywords:*
$LiCoO_2$ thin films
Lithium microbattery
Cycling properties
High specific capacities
RF sputtering

## ABSTRACT

$LiCoO_2$ thin films have been prepared on aluminium substrate with RF sputtering using a bias effect combined with a moderate post-annealing treatment at 500 °C and their electrochemical properties investigated in liquid electrolyte by cyclic voltammetry, galvanostatic experiments in various voltage windows, and ac impedance spectroscopy. The positive effect of bias is shown allowing to minimize the presence of the cubic $LiCoO_2$ phase. The lithium extraction process is highly reversible in the biased $LiCoO_2$ films with charge–discharge curves which really superimpose at C/10 rate. A 450 nm thin film is shown to exhibit an initial charge capacity of ≈60 μAh $cm^{-2}$ $\mu m^{-1}$ at C/10 and a high discharge capacity of ≈50 μAh $cm^{-2}$ $\mu m^{-1}$. The rate capability study demonstrates the film can easily sustain high charge–discharge rates and exhibits good cycling properties with capacity retention of 90% after 50 cycles up to a 2C rate and still 73% of the maximum capacity is recovered at 8C in the 4.2 V–3 V potential window. This constitutes remarkable performances both in terms of rate capability and cycling stability. The charge–discharge behaviour as a function of the film thickness in the range 0.25–3.6 μm is investigated and indicates an efficient and homogeneous electrochemical activity with a linear increase of the capacity with thickness. As a consequence an optimization of the capacity is proposed with the use of the thickest deposit of 3.6 μm leading to the value of 200 μAh $cm^{-2}$, the best one available for a $LiCoO_2$ film in liquid electrolyte.



## 1. Introduction

The development of all-solid-state thin film batteries is known to provide a suitable alternative to conventional rechargeable batteries because they can be incorporated into integrated circuits with other electronic elements. For instance, they have great interest for use in microsystems such as smart cards, on-chip power sources, lab-on-chip applications and portable electronic devices. High performance thin film cathodes are one of the requirements for a successful development of microbatteries. Due to its high specific capacity (140 mAh $g^{-1}$), high operating voltage (≈4 V), long cycle life and ease of preparation involving a heat treatment at temperature above 700 °C, the well-known and commonly used cathode material $LiCoO_2$ has been thoroughly investigated as thin film cathode. Among the various methods including radio frequency (RF) sputtering [1–24], pulsed laser deposition (PLD) [25–30], chemical vapour deposition (CVD) [31–34], spray pyrolysis [35–37], sol–gel processes [38–41] and electrochemistry [42,43],

* Corresponding author. Tel.: +33 149781155; fax: +33 149781148.
*E-mail addresses:* baddour@impe.cnrs.fr, baddour@glvt-cnrs.fr (R. Baddour-Hadjean).
[1] Present address: Volvo Group Trucks Technology, Advanced Technology and Research, Sven Hultins Gata 9D, 41288 Gothenburg, Sweden.

0378-7753/$ – see front matter © 2013 Elsevier B.V. All rights reserved.
http://dx.doi.org/10.1016/j.jpowsour.2013.06.047

DC or RF sputtering is the most widely used technique to perform thin film deposits of this cathode material. The challenge for the synthesis of high performance $LiCoO_2$ thin films is to obtain the well crystallized hexagonal structure by using a low temperature heat-treatment, lower than the usual 700 °C annealing, in order to allow the direct integration of the battery in specific devices and the use of low-temperature substrates.

Of course many studies report on the influence of some deposition parameters on the oxide film quality, both in terms of structure, morphology and electrochemical properties. These deposition parameters include the power, the temperature substrate, the nature of the working pressure (Ar, $O_2$, $Ar/O_2$), the working pressure, the $Ar/O_2$ ratio, the post-annealing treatment etc. In all cases one seeks to control the appropriate experimental parameters to optimize the crystallinity of the deposit and to promote the hexagonal HT-$LiCoO_2$ phase at the expense of the cubic LT-$LiCoO_2$ phase, the latter exhibiting poor electrochemical properties.

A few years ago preliminary results on deposited films with a bias substrate, which allows enhancing the surface mobility of the film-forming particles in the plasma, already indicated promising electrochemical properties in solid electrolytes [18]. However and surprisingly this effect of a bias substrate on the electrochemical performance has never been investigated combined with a post-annealing treatment. Structural data on annealed films confirm the interest of a substrate bias as additional process parameter to get the HT-$LiCoO_2$ phase [19]. In spite of numerous studies, cycling data available for sputtered $LiCoO_2$ thin films in liquid electrolytes are scarce and indicate rather poor properties with important capacity decay in the range 15–35% after 50 cycles [15,17,20,23].

More recently, we have reported from a detailed Raman study the promoting effect of the combined use of a negative substrate bias (50 V), an optimized value of the working pressure (>2 Pa) and a moderate heat-treatment temperature of 500 °C to strongly reduce the presence of cubic $LiCoO_2$ and $Co_3O_4$ phases to the benefit of the well crystallized hexagonal structure [44]. The present work reports for the first time the electrochemical properties of bias sputtered $LiCoO_2$ thin films in liquid electrolyte. The electrochemical efficiency of the films is investigated as a function of the thickness, from 0.25 μm to 3.6 μm, this crucial point being rarely addressed in previous works. In this paper, we show that bias sputtered $LiCoO_2$ thin films exhibit the best electrochemical performance in liquid electrolyte in terms of specific capacity, rate capability and capacity retention upon cycling.

## 2. Experimental

$LiCoO_2$ films with a thickness in the range 0.25–3.6 μm were deposited by radio frequency magnetron sputtering, using an ALCATEL SCM 600 reactor. The 150 mm target was made of 99.9% pure $LiCoO_2$ (SCI engineered materials). Aluminium foils (Goodfellow, purity 99,0%) with thickness of 200 μm were used as substrates. The target power was set to 500 W, the $Ar/O_2$ ratio to 3 and the total amount of gases was set to 53 sccm. The distance between target and substrate was 9.5 cm. The working pressure was fixed at 2.2 Pa. The deposition was made with a negative substrate bias voltage of 50 V. The deposited films were post-annealed in air at 500 °C for 2 h with a rate of 5 °C $min^{-1}$ and cooled to room temperature with a rate of 2 °C $min^{-1}$. The film thickness was determined with a Tencor AlphaStep 500 profilometer. Morphology and surface aspects of the films were observed with a Scanning Electron Microscope (SEM) LEO 1530 FEG. X-ray diffraction experiments were performed using a Bruker D8 Advance diffractometer with Cu K$\alpha$ radiation.

Raman microspectrometry experiments were performed with a LaBRAM HR 800 (Jobin–Yvon–Horiba) Raman micro-spectrometer including Edge filters and equipped for signal detection with a back illuminated charge coupled device detector (Spex CCD) cooled by Peltier effect to 200 K. A He:Ne laser (632.8 nm) was used as the excitation source. The spectra were measured in back-scattering geometry. The resolution was about 0.5 $cm^{-1}$. A 100× objective lens was used to focus the laser light on sample surface to a spot size of 1 $\mu m^2$. To avoid local heating of the sample, the power of the laser beam was adjusted to 0.2–0.5 mW with neutral filters of various optical densities. Raman spectra have been recorded on 15 different spots of each thin film electrode. The Raman spectra have been examined using deconvolution analysis of data sets exhibiting multiple peaks.

Electrodes of 14 mm in diameter were assembled in coin-type cells (CR2032), with metallic lithium as counter electrode, filled in with a commercial grade LP30 electrolyte (Merck) 1 M $LiPF_6$

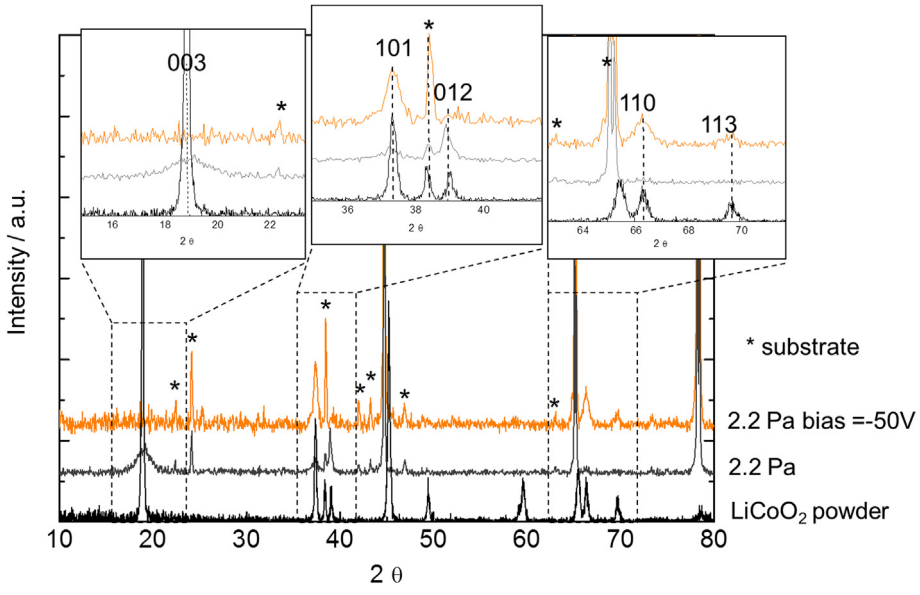


**Fig. 1.** XRD measurements of 450 nm thick films deposited at 2.2 Pa with or without a negative bias substrate of 50 V and post-annealed at 500 °C. *Substrate peaks.

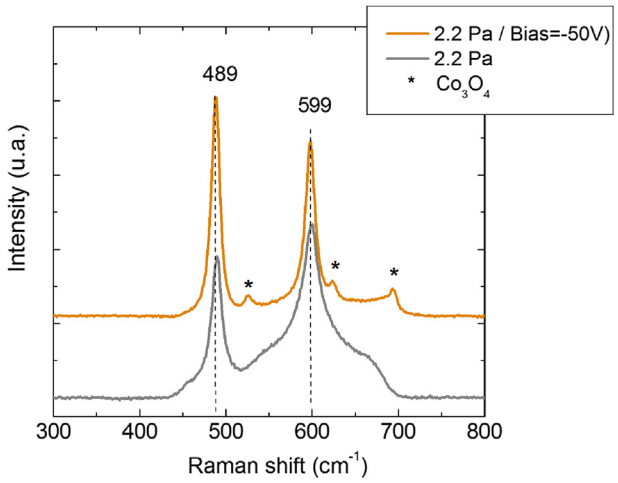


**Fig. 2.** Raman spectra of 450 nm $LiCoO_2$ thick films deposited at 2.2 Pa with or without a −50 V bias substrate and post-annealed at 500 °C. LT: low temperature *Fd3m* phase; HT: high temperature *R-3m* phase.

(EC:DMC = 1:1). The separator is constituted by a Viledon® membrane soaked with electrolyte and Cellgard®. Galvanostatic experiments were made with a multichannel VMP3 apparatus (BioLogic Science Instruments).

## 3. Results and discussion

In general, the crystallinity of the $LiCoO_2$ deposit as well as the cubic/hexagonal relative amounts are the critical factors for determining cell capacity and good cyclability. We have previously demonstrated that the experimental parameters allowing to meet such requirements are: a high working pressure of 2.2 Pa combined with a substrate bias of −50 V and a moderate heat-treatment at 500 °C. As a matter of fact, the content of the cubic phase is strongly reduced, in such optimized thin films (<10% by weight) [44]. Fig. 1 shows the XRD patterns of 450 nm $LiCoO_2$ thick films deposited with or without a bias procedure and that of a $LiCoO_2$ powder for comparison. All the diffraction patterns can be indexed on the basis of a hexagonal symmetry with unit cell parameters $a = b = 2.82$ Å and $c = 14.05$ Å of the $LiCoO_2$ phase (*R-3m* space group). The broadness of the lines indicates small crystallite size. It is clear that the bias process influences the preferential orientation. Indeed, the (*003*) and (*012*) lines disappear to the benefit of the (*101*) and (*110*) diffraction peaks when a bias is applied. The preferential (*110*) orientation is reported to be more favourable for fast Li diffusion than the (*003*) one [6].

As the *R-3m* and *Fd3m* XRD patterns are very close, (*018*)/(*110*) and (*006*)/(*012*) peaks splitting is the sole evidence for the presence of the *R-3m* HT-$LiCoO_2$ phase, and due to the broadness of the peaks, X-ray diffraction does not enable a clear assignment of the $LiCoO_2$ structure in the deposited films. However, Raman microspectrometry has been shown to discriminate between the hexagonal and the cubic phase and to give an evaluation of the relative amount of both compounds [44]. Fig. 2 outlines the positive effect of the bias polarization, as shown by the strong decline of the Raman *Fd3m* contribution which decreases from 40% without bias to less than 10% with a bias value of −50 V [44]. This low content in cubic phase was directly correlated to the electrochemical performances, a large increase of the capacity value as well as an improvement of the cycling properties being demonstrated for the pure LiCoO2 film [44].

Fig. 3 illustrates the morphology of the corresponding film. The SEM images indicate a crack free surface with a homogeneous grain size distribution of particles of about 100 nm which clearly increases due to the bias effect. A porosity of the film deposit is then observed. The cross section of the same dense film deposited on a Si substrate shows a columnar growth perpendicular to the substrate surface.

As shown by the typical charge–discharge curves at C/10 reported in Fig. 4a, the 450 nm thick film exhibits a high capacity value of 59 μAh $cm^{-2}$ $\mu m^{-1}$ close to the theoretical one in the initial charge and a rapid stabilization of the discharge capacity around 50 μAh $cm^{-2}$ $\mu m^{-1}$ after a few cycles. This typical electrochemical fingerprint of the HT-$LiCoO_2$ phase is confirmed by the cyclic voltammetric curves (Fig. 4b) showing well defined and reversible anodic and cathodic peaks at 3.90 V followed by shoulders at 4.08 and 4.17 V. When a sweeping rate of 20 μV $s^{-1}$ is applied, 94% of the charge capacity is still recovered in the discharge process, showing the highly rechargeable character of the thin film cathode. In addition, the cyclic voltammetric curves for the first two cycles remarkably superimpose which suggests a promising cycle life can be expected.

Fig. 5 displays the evolution of the film capacity versus cycle number at C/2.5 (10 μA $cm^{-2}$) and 2C (50 μA $cm^{-2}$) rate in the 4.2 V–3 V potential range. As a first outstanding observation, it can be seen the capacity value is little affected by the current density and decreases very slowly from about 50 to 45 μAh $cm^{-2}$ $\mu m^{-1}$ after 60 cycles at C/2.5, which corresponds to a capacity retention of 90%. Very close values are achieved at 2C. Such a stability has never been reached as yet with sputtered $LiCoO_2$ films annealed at a relatively low temperature of 500 °C and even overpasses the one reported for deposits annealed at 700 °C. For instance, for a 500 °C annealed film, C. L. Liao et al. [20,21] report the discharge capacity rapidly drops from 42 to 24 μAh $cm^{-2}$ $\mu m^{-1}$ after 50 cycles at 10 μA $cm^{-2}$, i.e. a capacity retention of only 57% against 90% in the present work. A better, but still limited, capacity retention (70%) is obtained when an annealing temperature of 700 °C is used [20] while Kim et al. indicate the capacity retention does not exceed 50% for annealing treatments between 650 and 900 °C [23]. The present cycling results confirm the interest of the bias deposited films since practically the same capacity values and capacity retention are achieved

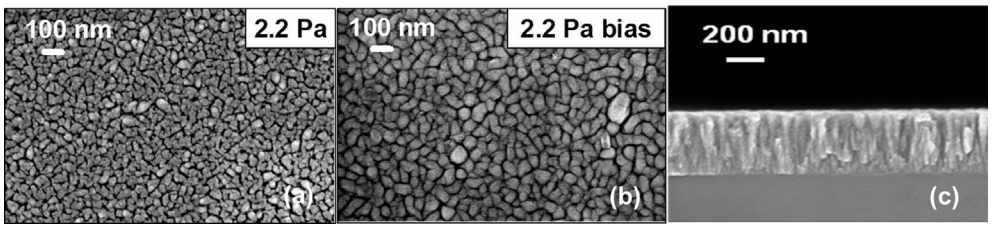


**Fig. 3.** SEM observation of the bias effect on the surface morphology of a 450 nm thick film deposited on Al substrate and post-annealed at 500 °C (a, b). Cross section of a biased film deposited on Si substrate (c).

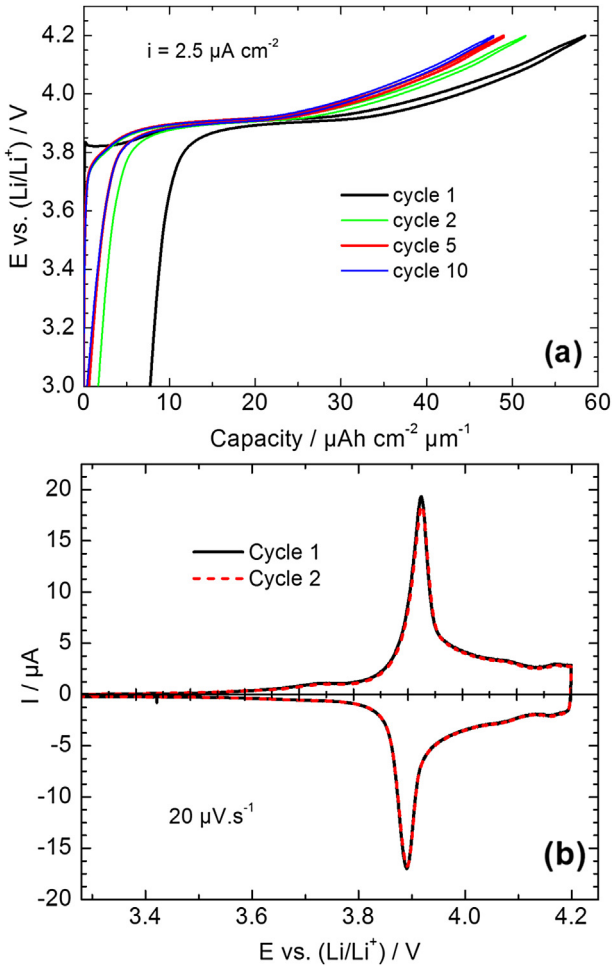


**Fig. 4.** (a) Charge–discharge curves of a 450 nm biased $LiCoO_2$ thin film at C/10 rate. Only cycles 1, 2, 5, 10 are reported. (b) Cyclic voltammetric curves at 20 µV $s^{-1}$.

when the rate increases to 2C (Fig. 5a). The charge–discharge profiles (Fig. 5b) indicate a lack of polarization during cycling while the similar capacity values recovered at C/2.5 and 2C illustrate the films are homogeneously deintercalated and intercalated. For CVD deposited $LiCoO_2$ films cycled in liquid electrolytes, it was observed that the film degrades rapidly and significantly during 50 cycles [33,34].

The rate capability has been investigated on the biased 450 nm $LiCoO_2$ thick film by applying galvanostatic cycling tests in the 4.2 V–3.4 V potential window with current densities increasing every 10 cycles from 2.5 µA $cm^{-2}$ to 5, 10, 50, 100, 200, 500 and 1000 µA $cm^{-2}$ i.e. from a C/10 rate to 40C. Sometimes a low current density of 10 µA $cm^{-2}$ is applied for 10 cycles to check whether the cathode film recovers its initial capacity. The typical fifth cycle is reported in Fig. 6 as a function of the current density. In the 2.5/100 µA $cm^{-2}$ range (from C/10 to 4C), both the capacity and the working voltage are little affected. The capacity decreases only by 10% and the mid-discharge voltage by ≈50 mV. A significant influence of the C rate only appears from 200 µA $cm^{-2}$ (8C) with a reasonable polarization phenomenon since the working potential is still high at 3.8 V. However, 83% of the maximum capacity is recovered at 4 C and still 73% at 8 C. Such results highlight the excellent rate capability of the bias deposited films post-annealed at moderate temperature.

Fig. 7 summarizes the influence of the current density on the capacity evolution with cycles. An impressive stability of the capacity is systematically achieved regardless of the current density. High values ranging from 47 to 38 µAh $cm^{-2}$ $µm^{-1}$ for C rates between C/10 and 8C. The film capacity sharply decreases only at 40C (1 mA $cm^{-2}$) to 20 µAh $cm^{-2}$ $µm^{-1}$ without damaging the film because the significant value of 47 µAh $cm^{-2}$ $µm^{-1}$ is recovered thereafter during subsequent cycling at C/2.5. These experiments clearly outline the excellent rate capability combined to attractive cycling properties of the bias sputtered $LiCoO_2$ thin film since the capacity decay is limited to only 4% after 100 cycles even after applying drastic changes in C rate. Let us recall that recovering the initial capacity of 47 µAh $cm^{-2}$ $µm^{-1}$ every 10 cycles at 10 µA $cm^{-2}$ shows the film deposit is not affected by this cycling procedure and successive C rate sequences. These results are the best one known for a sputtered thin film $LiCoO_2$ in liquid electrolyte.

In an attempt to optimize the specific capacity available, we have evaluated the discharge–charge properties of the film at C/2.5 in the various enlarged potential windows 3 V–4.3 V, 3 V–4.4 V and 3 V–4.5 V (Fig. 8). The upper limit of 4.3 V allows a capacity increase of 10% combined with a good stability. For 4.4 V, a further gain in capacity is obtained but at the expense of a slight decay with cycles. This latter trend is more pronounced if a cutoff voltage of 4.5 V is applied. In addition, for the highest voltage limits of 4.4 and 4.5 V, the coulombic efficiency is seen to decrease with a higher charge capacity, probably due to irreversible structural changes combined with an increasing contribution of electrolyte decomposition.

One way for obtaining high capacity values in the 3 V–4.2 V potential window consistent with the structural stability of $LiCoO_2$ is to increase the film thickness. Fig. 9a summarizes the typical second charge–discharge cycle achieved at 10 µA $cm^{-2}$ for bias sputtered thick films in the range 0.450 µm–3.6 µm. The capacity is

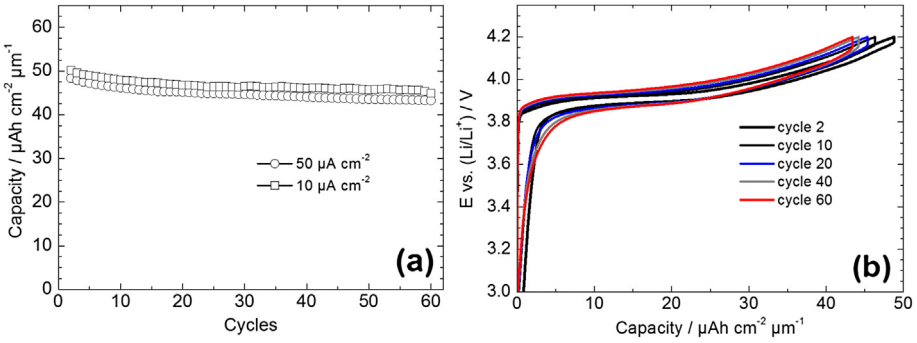


**Fig. 5.** (a) Evolution of the specific capacity versus cycle number for cycling galvanostatic experiments performed on a 450 nm biased $LiCoO_2$ film at C/2.5 and 2C rate in the 4.2/3 V potential range; (b) Charge–discharge profiles vs. cycles for a 450 nm biased $LiCoO_2$ film at 2 C in the 4.2/3 V potential range.

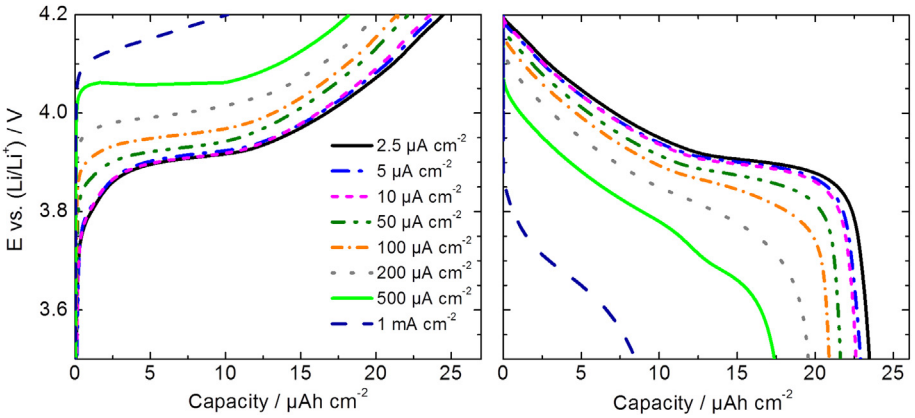


**Fig. 6.** Influence of the current density on the charge–discharge performance of a 450 nm, biased $LiCoO_2$ film.

seen to increase with the thickness without any polarization to reach a high value of about 210 µAh $cm^{-2}$ $µm^{-1}$ in charge and 200 µAh $cm^{-2}$ $µm^{-1}$ for discharge for the thickest film.

In order to completely characterize the rate capability of these various thin films, constant-current discharge–charge cycles were performed at C/10, C/7, C/3.5, C, 2C and 5C. The results obtained for all the samples are summarized in Fig. 9b. The specific capacity linearly increases with the thickness from 10 µAh $cm^{-2}$ for 0.25 µm to 210 µAh $cm^{-2}$ for 3.6 µm. Except for the thickest film, it is of interest to note that, regardless of the film thickness, the achieved specific capacities are practically not dependent on the current density up to 2C, which indicates the kinetics of lithium transport into these sputtered films is very high. At 2C and 5C and for film thicknesses ≥1.8 µm, the electrochemical response, i.e., the capacity vs thickness is no more linear, probably due to important kinetic effects which probably prevail in the thickest films at high C-rate. However, 60% of the maximum capacity is still achieved for the 1.8 µm thick film.

In summary, the thickness dependence of the capacity for various discharge–charge rates can be represented by a straight-line (Fig. 9b). Such an electrochemical response of the bias $LiCoO_2$ films demonstrates their high electrochemical efficiency which can be explained by a homogeneous and fast Li diffusion in all $LiCoO_2$ particles, a good adherence ensuring a good electronic contact to the substrate and probably a sufficient porosity to ensure a good contact between electrolyte and particles of active material.

High specific capacities of ≈200 µAh $cm^{-2}$, as reported in Fig. 10, are the highest values known for sputtered $LiCoO_2$ films in liquid electrolytes. Higher values of about 250 µAh $cm^{-2}$ have been previously reported for thicker films of 6.2 µm prepared by electron cyclotron resonance (ECR) sputtering which exhibit however a lower electrochemical efficiency [24]. In other respects, capacities up to 300 µAh $cm^{-2}$ have been obtained in all-solid-state

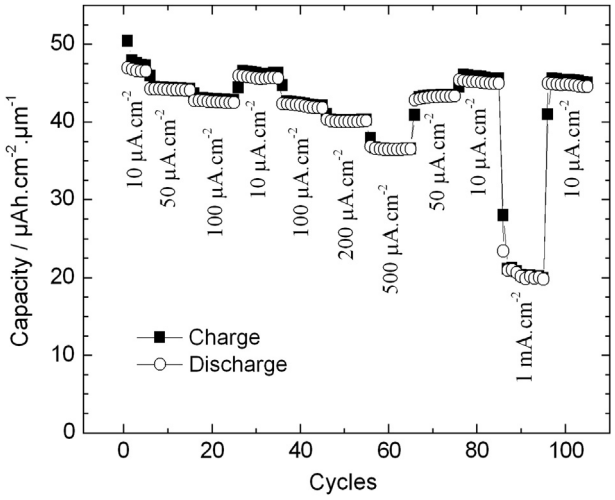


**Fig. 7.** Evolution of the specific capacity during cycling as a function of the current density for a biased 450 nm $LiCoO_2$ film.

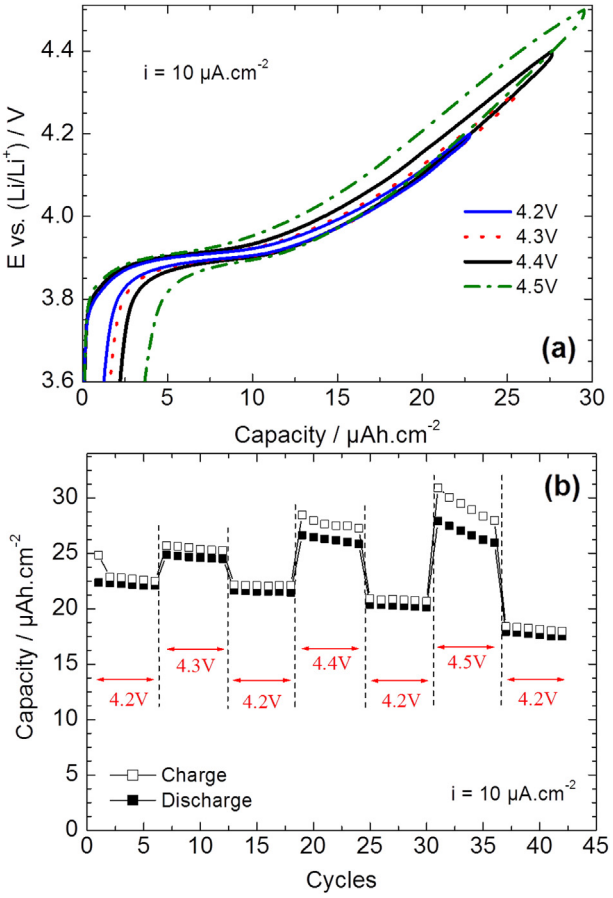


**Fig. 8.** Influence of the upper voltage limit on the cycling performance of a 450 nm biased $LiCoO_2$ film at C/2.5 rate.

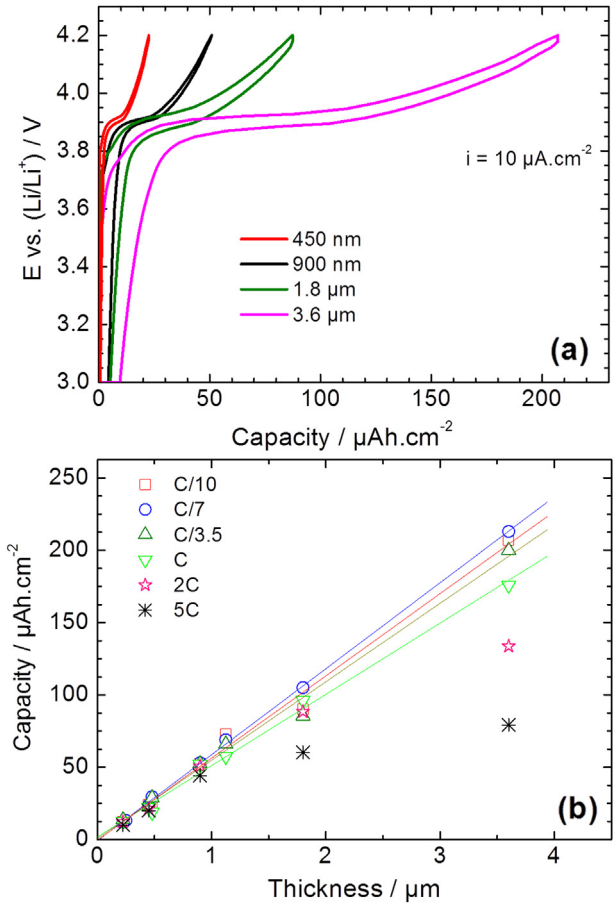


**Fig. 9.** Influence of the film thickness on the charge–discharge curves at 10 µA $cm^{-2}$ of bias deposited $LiCoO_2$ (a). Rate capability study as a function of film thickness (b).

microbatteries for sputtered 4.2 µm thick films but requiring a post-annealing treatment at a higher temperature of 700 °C [2].

To obtain further insight into the kinetics parameters that control the lithium intercalation reaction into the biased $LiCoO_2$ films, ac impedance measurements have been carried out as a function of the charge potential in the frequency range $2 \times 10^5$ Hz–

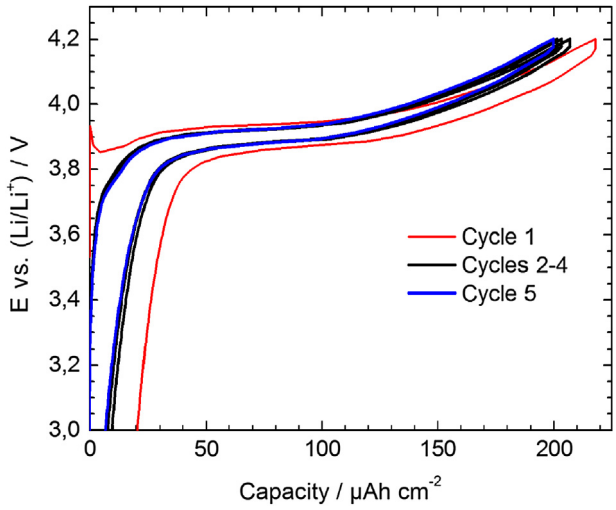


**Fig. 10.** Cycling curves at C/2.5 rate for the thickest film (3.6 µm).

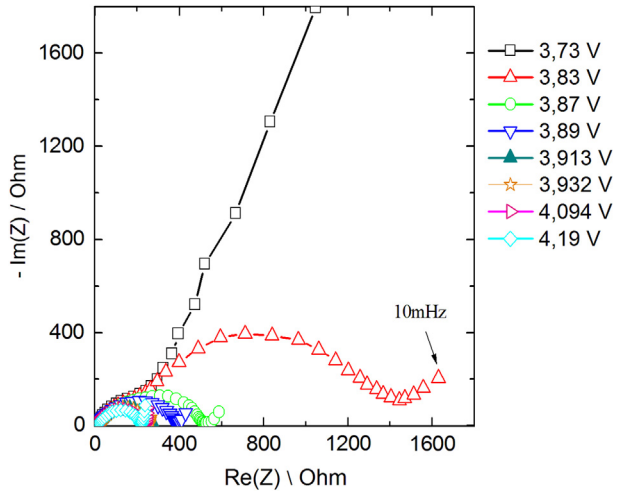


**Fig. 11.** Potential dependence of the Nyquist diagram for a $LiCoO_2$/Li cell for Li extraction.

$10^{-2}$ Hz. Fig. 11 reports the Nyquist diagrams obtained at each voltage for the 450 nm thick film. The contribution of the Li anode is negligible and probably constant in this potential range, as previously reported for PVD $LiCoO_2$ thin films [6].

The first diagram obtained at 3.73 V is characterized by the lack of semi-circle and a high impedance value. Then, lithium deintercalation provokes an immediate and huge decrease of the cell impedance up to 3.87 V which continues to decrease more slowly with higher values of potential. A well defined semi-circle seems to be more and more defined with deintercalation and could be ascribed in a first approach to the charge-transfer resistance. Fig. 12 shows that the cathode impedance considerably drops when the electrode potential increases to rapidly stabilize from 3.90 V. Such a finding has been also observed for sputtered films and porous electrode [6,45]. This trend is probably related to the increase in electronic conductivity as it is known that $LiCoO_2$ changes from semiconducting to conducting in the first stages of the deintercalation [6,46].

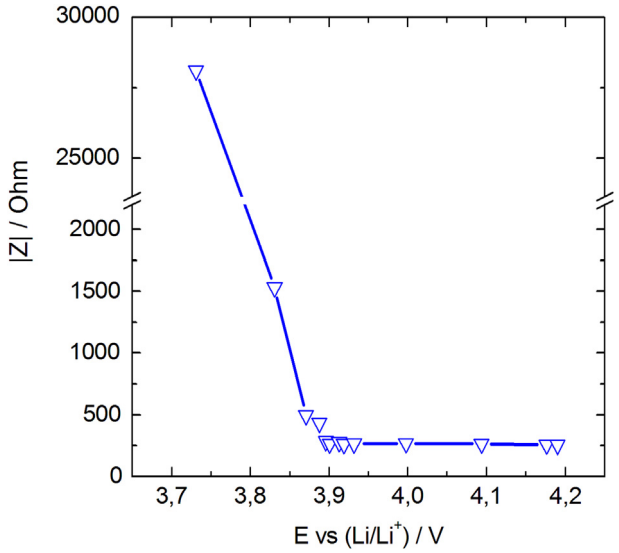


**Fig. 12.** Evolution of the cell impedance vs voltage for Li extraction from a biased sputtered $LiCoO_2$ film.

## 4. Conclusions

Combining a high working pressure, a bias effect and a moderate post-annealing treatment at 500 °C, high performance $LiCoO_2$ thin films have been prepared using RF sputtering in a wide range of thickness 0.25–3.6 μm. We show that a 450 nm thick film can work without any polarization at 2C rate, delivering then a specific capacity of ≈50 μAh $cm^{-2}$ $\mu m^{-1}$ with a capacity retention of 90% after 50 cycles. This finding is remarkable when compared to the capacity retention of 50–70% usually achieved with sputtered films regardless of the post-annealing temperature. The present biased $LiCoO_2$ films constitute high rate cathode materials since 83% of the maximum capacity is recovered at 4 C and still 73% at 8 C. Moreover, the films can sustain up to 40 C without damaging its further cycling behaviour. Such attractive electrochemical characteristics have never been reported as yet. The experimental procedure to produce such sputtered films has been proven to be highly reliable and reproducible, as shown by the linear increase of capacity with thickness over the range 0.25–3.6 μm. This allows capacities as high as 200 μAh $cm^{-2}$ to be reached with a 3.6 μm thick film. This capacity value is the highest known as yet in liquid electrolytes.

In a few words we demonstrate the bias effect is the key parameter to get high performance sputtered $LiCoO_2$ films characterized by a high electrochemical efficiency, a high rate capability and good cycling properties. Hence, biased $LiCoO_2$ films answer the crucial challenge for all solid-state batteries of decreasing the post-annealing temperature from 700 °C to 500 °C or 400 °C. Our preliminary works with LiPON solid electrolyte have been performed and indicate an excellent stability of the capacity of 50 μAh $cm^{-2}$ $\mu m^{-1}$ over at least 140 cycles [47].

## References


[1] B. Wang, J.B. Bates, F.X. Hart, B.C. Sales, R.A. Zuhr, J.D. Robertson, J. Electrochem. Soc. 143 (1996) 3203.
[2] N.J. Dudney, Y.I. Jang, J. Power Sources 119–121 (2003) 300.
[3] J.B. Bates, N.J. Dudney, B.J. Neudecker, F.X. Hart, H.P. Jun, S.A. Hackney, J. Electrochem. Soc. 147 (2000) 59.
[4] J.B. Bates, N.J. Dudney, B. Neudecker, A. Ueda, C.D. Evans, Solid State Ionics 135 (2000) 33.
[5] P.J. Bouwman, B.A. Boukamp, H.J.M. Bouwmeester, H.J. Wondergem, P.H.L. Notten, J. Electrochem. Soc. 148 (2001) A311.
[6] P.J. Bouwman, B.A. Boukamp, H.J.M. Bouwmeester, P.H.L. Notten, J. Electrochem. Soc. 149 (2002) A699.
[7] J.F. Whitacre, W.C. West, B.V. Ratnakumar, J. Power Sources 103 (2001) 134.
[8] J.K. Lee, S.J. Lee, H.K. Baik, H.Y. Lee, S.W. Jang, S.M. Lee, Electrochem. Solid State Lett. 2 (1999) 512.
[9] M. Hayashi, M. Takahashi, Y. Sakurai, J. Power Sources 174 (2007) 990.
[10] J.F. Whitacre, W.C. West, E. Brandon, B.V. Ratnakumar, J. Electrochem. Soc. 148 (2001) A1078.
[11] K.F. Chiu, F.C. Hsu, G.S. Chen, M.K. Wu, J. Electrochem. Soc. 150 (2003) A503.
[12] J. Pracharova, J. Pridal, J. Bludska, I. Jakubec, V. Vorlicek, Z. Malkova, Th. Dikonimos Makris, R. Giorgi, L. Jastrabik, J. Power Sources 108 (2002) 204.
[13] X. Zhu, Z. Guo, G. Du, P. Zhang, H. Liu, Surf. Coat. Technol. 204 (2010) 1710.
[14] S.W. Jeon, J.K. Lim, S.H. Lim, S.M. Lee, Electrochim. Acta 51 (2005) 268.
[15] H. Pan, Y. Yang, J. Power Sources 189 (2009) 633.
[16] H.Y. Park, S.C. Nam, Y.C. Lim, K.G. Choi, K.C. Lee, G.B. Park, H.P. Kim, S.B. Cho, Korean J. Chem. Eng. 23 (2006) 832.
[17] C. Ziebert, B. Ketterer, M. Rinke, C. Adelhelm, S. Ulrich, K.-H. Zum Gahr, S. Indris, T. Schimmel, Surf. Coat. Technol. 205 (2010) 1589.
[18] H.Y. Park, S.R. Lee, Y.J. Lee, B.W. Cho, W.I. Cho, Mater. Chem. Phys. 93 (2005) 70.
[19] B. Ketterer, H. Vasilchina, K. Seeman, S. Ulrich, H. Besser, W. Pfleging, T. Kaiser, C. Adelhelm, Int. J. Mater. Res. 99 (2008) 1171.
[20] C.L. Liao, K.Z. Fung, J. Power Sources 128 (2004) 263.
[21] C.L. Liao, Y.H. Lee, K.Z. Fung, J. Alloys Compd. 436 (2007) 303.
[22] J. Xie, N. Imanishi, T. Matsumura, A. Hirano, Y. Takeda, O. Yamamoto, Solid State Ionics 179 (2008) 362.
[23] W.S. Kim, J. Power Sources 134 (2004) 103.
[24] M. Takahashi, M. Hayashi, Y.T. Shodai, J. Power Sources 189 (2009) 191.
[25] M. Antaya, J.R. Dahn, J.S. Preston, E. Rossen, J.N. Reimers, J. Electrochem. Soc. 140 (1993) 575.
[26] K.A. Striebel, C.Z. Deng, S.J. Wen, E.J. Cairns, J. Electrochem. Soc. 143 (1996) 1821.
[27] J.D. Perkins, C.S. Bahn, J.M. Mc Graw, P.A. Parilla, D.S. Ginley, J. Electrochem. Soc. 148 (2001) A1302.
[28] C. Julien, M.A. Camacho-Lopez, L. Escobar-Alarcon, E. Haro-Poniatowski, Mater. Chem. Phys. 68 (2001) 210.
[29] S.B. Tang, M.O. Lai, L. Lu, J. Alloys Compd. 424 (2006) 342.
[30] H. Xia, L. Lu, Electrochim. Acta 52 (2007) 7014.
[31] S.I. Cho, S.G. Yoon, J. Electrochem. Soc. 149 (2002) A1584.
[32] S.I. Cho, S.G. Yoon, Appl. Phys. Lett. 82 (2003) 3345.
[33] W.-G. Chai, S.-G. Yoon, J. Power Sources 125 (2004) 236.
[34] J.F.M. Oudenhoven, T. Van Dongen, R.A.H. Niessen, M. de Croon, P.H.L. Notten, J. Electrochem. Soc. 156 (2009) D169.
[35] P. Fragnaud, T. Brousse, D.M. Schleich, J. Power Sources 63 (1996) 187.
[36] P. Fragnaud, R. Nagarajan, D.M. Schleich, D. Vujic, J. Power Sources 54 (1995) 362.
[37] Y. Yu, J.L. Shui, Y. Jin, C.H. Chen, Electrochim. Acta 51 (2006) 3292.
[38] Y.H. Rho, K. Kanamura, T. Umegaki, J. Electrochem. Soc. 150 (2003) A107.
[39] Y.H. Rho, K. Kanamura, M. Fujisaki, J.I. Hamagami, S.I. Suda, T. Umegaki, Solid State Ionics 151 (2002) 151.
[40] M.K. Kim, H.T. Chung, Y.J. Park, J.G. Kim, J.T. Son, K.S. Park, H.G. Kim, J. Power Sources 99 (2001) 34.
[41] H. Porthault, F. Le Cras, S. Franger, J. Power Sources 115 (2010) 6262.
[42] H. Porthault, F. Le Cras, R. Baddour-Hadjean, J. P Pereira-Ramos, S. Franger, Electrochim. Acta 56 (2012) 7580.
[43] K.S. Han, S.W. Song, S. Tsurimoto, H. Fujita, I. Sasagawa, K.H. Choi, H.K. Kang, M. Yoshimura, Solid State Ionics 151 (2002) 11.
[44] S. Tintignac, R. Baddour-Hadjean, J.P. Pereira-Ramos, R. Salot, Electrochim. Acta 60 (2012) 121.
[45] M.D. Levi, G. Salitra, B. Markovsky, H. Teller, D. Aurbach, U. Heider, L. Heider, J. Electrochem. Soc. 146 (1999) 1279.
[46] J. Molenda, A. Stoklosa, T. Bak, Solid State Ionics 36 (1989) 53.
[47] C. Navone, S. Tintignac, J.P. Pereira-Ramos, R. Baddour-Hadjean, R. Salot, Solid State Ionics 192 (2011) 343.